

Jean-Nicolas Ouellet · Patrick Hébert

## Precise ellipse estimation without contour point extraction

Received: date / Accepted: date

**Abstract** This paper presents a simple linear operator that accurately estimates the parameters of ellipse features. Based on the dual conic model, the operator directly exploits the raw gradient information in the neighborhood of an ellipse's boundary, thus avoiding the intermediate stage of precisely extracting individual edge points. Moreover, under the dual representation, the dual conic can easily be constrained to a dual ellipse when minimizing the algebraic distance. The new operator is compared to other estimation approaches, including those limited to the center position, in simulation as well as in real situation experiments.

**Keywords** ellipse targets · conic · dual conic · dual ellipse · geometric fitting · Forstner operator

---

Jean-Nicolas Ouellet

Laval University

Canada (Qc), Quebec

G1K 7P4

Tel.: +1-418-656-2131-4786

Fax: +1-418-656-3594

E-mail: [jouellet@gel.ulaval.ca](mailto:jouellet@gel.ulaval.ca)

Patrick Hébert

Laval University

Canada (Qc), Quebec

G1K 7P4

Tel.: +1-418-656-2131-4479

Fax: +1-418-656-3594

E-mail: [hebert@gel.ulaval.ca](mailto:hebert@gel.ulaval.ca)

## 1 Introduction

Precise estimation of an ellipse in an image usually consists in accurately extracting contour points with subpixel precision before fitting ellipse parameters on the obtained set of points. Until recently, numerous methods have been proposed for fitting an ellipse from a given set of contour points [2–4, 6, 12, 13, 16]. They differ from each other depending on their precision, accuracy, robustness to outliers or on their ability to fit parameters on partial ellipse contours. All these methods rely on a set of contour points that are extracted beforehand. Nevertheless, extracting contour points usually subsumes multiple stages including gradient estimation, non-maximum suppression, thresholding, and subpixel estimation.

Extracting contour points imposes making a decision for each of those points based on neighboring pixels in the image. The following question thus arises. Is it possible to develop a more direct method that precludes the extraction of a set of contour points? One would directly exploit the information encoded in all pixels in the ellipse neighborhood. By eliminating precise contour point extraction, the method would be greatly simplified and the uncertainty on the recovered ellipse parameters will be assessed more closely to the image data. Another motivation for developing such an approach is the possibility to process low contrast images where each contour point can hardly be extracted along the ellipse.

Formally, given a set of pixels nearby an complete ellipse contour in a real image, what are the ellipse parameters? Although the limitation to complete ellipses might appear restrictive, it is of great interest for camera calibration and precise measurement applications where it is common to use physical circular targets that project into ellipses in an image [10]. In these applications, partial ellipses lead to a less reliable estimation and are generally avoided. In Fig. 1(a), a rectangular area enclosing an ellipse is shown. We develop a method that can accurately fit the ellipse’s parameters from all the pixels that lie inside such an area or preferably nearby the ellipse’s contour. More precisely, we will show how one can estimate the ellipse’s parameters directly from the gradient vector field. Fig. 1(c) is a close up view where the gradient vector field as well as the fitted ellipse contour are superimposed on the image. It is important to note that we focus on ellipse parameter estimation, as opposed to ellipse detection. Although their detection is simple from calibration targets, in more general situations it is assumed that the set of pixels describing an ellipse can be roughly identified beforehand.

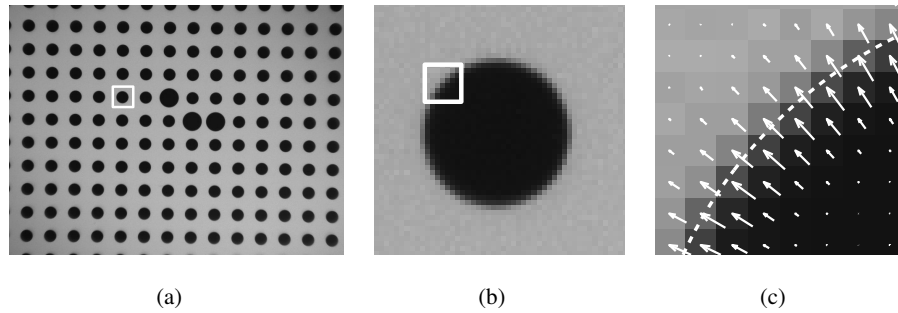


**Fig. 1** (a) Complete image of a calibration target. The marked region indicates the pixels contributing to the ellipse estimation. (b) Close-up view of the marked region. (c) Close-up view of the region identified in (b) where the image gradient orientation and magnitude is represented by arrows superimposed on the image. A dotted line depicts the fitted ellipse contour.

The most relevant work to ours is that of Forstner who developed an operator for extracting circular and corner features in an image [5]. In this extraction process, detection is also decoupled from estimation. For localizing circular features, the detection of contour points is avoided by directly processing the gradient components of the image in the neighborhood of a detected feature. In this paper, we show how it is possible to extend the basic principle for the estimation of ellipse parameters. For that purpose, we will exploit the dual conic model and we will show that one can easily constrain the dual conic to a dual ellipse. The resulting linear algorithm is of remarkable simplicity and provides results at least as precise and accurate as the best methods. It also makes it possible to fit ellipses in images where individual contour points would be unreliable.

In [15], the authors introduced the dual ellipse operator as an extension of the Forstner operator. This current paper provides more details on the method and completes the analysis of the algebraic error in the dual space. Moreover, a new series of experiments in simulation on partial ellipses as well as in challenging cases taken from natural images is presented. In the sequel, a review of widely used methods for estimating ellipse parameters, including those limited to center position estimation, is first presented. Then, Forstner's original method is described before developing the new operator in Section 3. Next, a series of comparative experiments for assessing the relative accuracy, precision and robustness to lighting conditions is presented in Section 4. The experiments conclude with a section where the operator is stressed in challenging conditions such as estimation from partial contours and ellipses occurring in natural images.

## 2 Related work

An ellipse can be estimated from the image intensity or its gradient. Intensity-based methods are also referred to as direct methods [18] when they directly exploit the image intensity with no transformation or derivation. One simple method which returns the coordinates of the feature is the gray-scale centroid, where for a given region, the intensity of each pixel is used to weigh its contribution to the estimation of the intensity center of mass. Integrating over all pixels in the region provides good immunity to noise. However, intensity-based methods like centroid estimation are particularly sensitive to non-uniform illumination. The causes of non-uniform illumination are frequent and various, e.g. light sources, vignetting or reflections on specular surfaces.

Gradient-based methods are less affected by non-uniform illumination. Nevertheless, the derivation process involved makes them more sensitive to noise. Generally, these latter methods are composed of two distinct steps; the edges of a region are first identified after non-maxima suppression and a conic is fitted to the edge points. The simplest method, linear least-square, minimizes the algebraic error associated with the points. Since the linear system is homogeneous, a constraint must be imposed on the conic parameters  $\Theta = [A, B, C, D, E, F]^T$  to avoid the trivial solution  $\Theta = \mathbf{0}$ . Many possible constraints were studied in order to estimate the best conic from a set of points, e.g.  $F = 1$ ,  $\|\Theta\| = 1$  (see [4, 16] for a review). Nevertheless, it is essential for a conic estimator to be invariant to Euclidean transformations (translation, rotation, scale) [1]. According to this definition the constraints  $\|\Theta\| = 1$  and  $F = 1$  are not invariant. On the other hand, the expression  $4AC - B^2$  is a conic invariant and can be formulated as the quadratic constraint  $4AC - B^2 = 1$ . Under this constraint, the parameters minimizing the algebraic error, which are obtained via a generalized eigensystem, describe elliptical shapes [3]. However, in the presence of partial ellipses, this method, and all other methods based on the algebraic error, will underestimate the eccentricity of the ellipse [20]. Different iterative algorithms were introduced to reduce or compensate for the bias [2, 12]. Still, given that ellipses are complete, the effect of the bias is practically nonexistent and there are no significant differences among high quality fitting methods [4]. In this situation, it is advantageous to employ the simplest method.

Estimating a conic from pixels' centers identified as local maxima is generally inaccurate. A better estimation is obtained from the edge points whose positions are known with subpixel precision. A simple way to achieve subpixel precision is to perform a parabolic interpolation of the gradient maximum along the edge direction. The method is simple but the interpolation is sensitive to noise. An alternative is proposed in [19]

where an ideal step edge is fitted to the image intensity value such that the first three sample moments are preserved. The fitting is done over a region centered at the gradient local-maximum which provides a larger fitting area, thus greatly reducing the sensitivity to noise. However, with this method, the location can be biased if the edge is curved inside the region. To reduce the bias in the presence of curved edges, a correction term based on the local curvature of the contour was proposed in [17] and later refined in [9]. This leads to even more complex methods. By contrast, a method directly exploiting the gradient in the region encompassing an ellipse could greatly simplify the location process.

A radically different approach was proposed by Forstner [5] for the localization of corners and circular features. In his approach, individual edge detection is avoided; the feature's location is estimated directly from the image gradient calculated in a region encompassing the feature. Actually, the gradient at a pixel in the neighborhood of a feature edge provides the orientation of a 2D line passing through the pixel center. The location of a feature is obtained by estimating the intersection point of a set of these lines in the feature's neighborhood. The operator can be adapted to locate corners, where the lines are oriented perpendicularly to the gradient and intersect at the corner location, or circle centers in which case the lines are oriented parallel to the gradient as shown in Fig. 2(a). The intersection point is estimated by means of least-squares where each line contributes with a weight set proportional to the squared magnitude of the gradient [5].

Although very simple and fast, the Forstner operator is not adapted to locate elliptical feature centers; the lines defined by the gradient on the boundary of an ellipse do not converge as shown in Fig.2(b). Since ellipses are more general and frequent in images, it is interesting to develop a new operator inspired by the same principle. Another motivation for improving the Forstner operator is to reduce the effect of the gradient orientation error hampering the operator. Actually, noise causes small angular errors in the gradient orientation. While the significance of orientation errors is small when locating corners, it is not the case for circle centers where the errors cause a leverage effect due to the distance between the edges and the intersection of the lines. As with corners, the operator should exploit observables, such as the contours, that directly characterize the feature. This suggests to exploit tangent lines and to apply the estimation in the dual space.

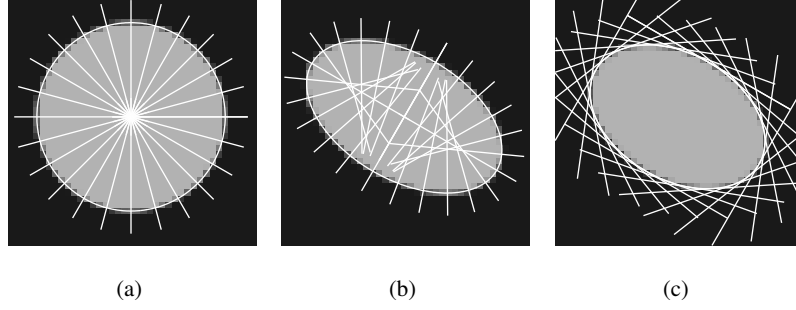


**Fig. 2** (a) Lines parallel to the circle gradient vectors intersect at the circle center. (b) Lines parallel to the ellipse gradient vectors are not convergent. (c) Lines perpendicular to the ellipse gradient vectors are tangent to the ellipse.

### 3 Description of the new operator

#### 3.1 Background on conic and dual conic

A conic is a planar curve formed by the intersection of a plane with a circular cone. Generally the term conic refers to a point conic, defining an equation on points. In projective geometry the role of homogeneous points and lines can be interchanged; this is known as the duality relationship. As a result, there is a dual conic (see Fig. 2(c)) which defines an equation on lines instead of points [8]. More precisely, a point,  $x_i = [u_i, v_i, 1]^T$ , in

homogeneous coordinates lies on the conic  $\mathbf{C} = \begin{bmatrix} A & \frac{B}{2} & \frac{D}{2} \\ \frac{B}{2} & C & \frac{E}{2} \\ \frac{D}{2} & \frac{E}{2} & F \end{bmatrix}$  iff it satisfies  $x_i^T \mathbf{C} x_i = 0$ . In a similar way a line

$l_i = [a_i, b_i, c_i]^T$  is tangent to the dual of conic  $\mathbf{C}$  iff it satisfies  $l_i^T \mathbf{C}^* l_i = 0$ . Here  $\mathbf{C}^*$  is the inverse matrix of  $\mathbf{C}$ , given full rank matrix. It is interesting to note that the dual conic center  $e_c = (u_c, v_c)$  is obtained directly from the parameters. Actually, if the pole of a line  $l$  is defined as a point  $x$  such that  $x = \mathbf{C}^* l$ , then the center of the dual conic is the pole of the line at infinity [11],

$$\lambda [u_c, v_c, 1]^T = \left[ \frac{D^*}{2}, \frac{E^*}{2}, F^* \right]^T = \mathbf{C}^* l_\infty. \quad (1)$$

Given a set of lines  $l_i$ , the parameter vector  $\Theta = \{A^*, B^*, C^*, D^*, E^*, F^*\}$  of the dual conic  $\mathbf{C}^*$  can be estimated by linear least-squares. The estimation is accomplished by finding  $\Theta$  for which  $\Phi(\Theta)$  reaches a minimum,

$$\Phi(\Theta) = \sum_{i \in R} \omega_i (l_i^T \mathbf{C}^*(\Theta) l_i)^2, \quad (2)$$

where  $R$  contains the set of lines contributing to the dual conic estimate and  $\omega_i$  is a weighting factor. Since  $l_i$  is a triplet of homogeneous coordinates, the scale of the lines is indeterminate. It can be fixed such that

$\|a, b\| = 1$ . Normal equations derived from Eq. (2) are linear in  $\Theta$  and lead to the following form:

$$\left[ \sum_{i \in R} \omega_i^2 K_i K_i^T \right] [\Theta] = \mathbf{0}, \quad (3)$$

where  $K_i$  is composed of line coefficients such that  $K_i = [a_i^2, a_i b_i, b_i^2, a_i c_i, b_i c_i, c_i^2]^T$ . This system can be solved under the constraint  $\|\Theta\| = 1$  using the singular value decomposition (SVD). However, this constraint is not invariant to Euclidean transformations [1]. A more appropriate constraint is introduced in the next section.

### 3.2 From dual conic to dual ellipse

The conic discriminant can be imposed as  $4AC - B^2 = 1$  as proposed in [3] to obtain an ellipse specific fitting.

From the duality relationship between points and lines, we know that a similar constraint can also be derived for the dual conic. Since a conic and its dual are related by the matrix inverse operation, the dual conic parameter  $F^*$  can be expressed in terms of the parameters of the conic  $\mathbf{C}$ :

$$F^* = \frac{1}{4|\mathbf{C}|} (4AC - B^2) = \frac{1}{|\mathbf{C}|} \begin{vmatrix} A & B/2 \\ B/2 & C \end{vmatrix}. \quad (4)$$

In this expression, the factor  $\frac{1}{4|\mathbf{C}|}$  can be canceled out since  $\mathbf{C}^*$  is known up to a scale factor. Hence, the conic discriminant  $4AC - B^2$ , which is strictly positive for ellipses [3], is intrinsically related to the term  $F^*$ . From Eq. 4, the ellipse condition in the dual space corresponds to  $F^* > 0$ . If the scaling of  $\mathbf{C}^*$  is incorporated into the condition, one obtains the dual ellipse fitting constraint  $F^* = 1$ . Then, the normal equations of the new system of five unknowns  $\Theta' = (A^*, B^*, C^*, D^*, E^*)$  hold the following matrix form:

$$\left[ \sum_{i \in R} \omega_i^2 K'_i K_i'^T \right] [\Theta'] = \sum_{i \in R} -\omega_i^2 K'_i c_i^2, \quad (5)$$

where  $K'_i$  is composed of the first five elements of  $K_i$ .

Although invariant to Euclidean transformations, the system could be sensitive to numerical error. Improving the conditioning of the equation system by means of data normalization will benefit the estimation process [7]. Line normalization is done by first shifting the origin of the coordinate system to an approximation of the center of the ellipse area and then scaling the axes such that the mean distance of the lines to the origin becomes  $\sqrt{2}$ .

### 3.3 Dual ellipse estimation from images

The image gradient near a contour naturally provides the orientation of the contour normal. Therefore, given a set of pixels belonging to the neighborhood of an ellipse, a set of lines can be constructed from the gradient to solve for Eq. (5). More precisely, when the image gradient  $\nabla I_i = [I_{ui}, I_{vi}]^T$  at a pixel  $x_i$  is not null, it defines the normal orientation of a line passing through the pixel center such that:

$$l_i = [I_{ui}, I_{vi}, -\nabla I_i^T x_i]^T. \quad (6)$$

From this definition, each line contributes with a weight equal to the squared gradient magnitude in Eq. (5). There are two advantages to give higher importance to observations where the gradient magnitude is strong. First, the operator will focus on the active zone of the gradient where the ellipse contour has high probability of being located. Thus, a precise interpolation step is not required, the operator processes all pixels. Second, the robustness to noise is improved, particularly in regions of weak gradient where the line orientation is not well defined.

The resulting operator requires very few steps and computations. Actually, each pixel of the region contributes to the sums in Eq. 5. Once the parameters are obtained, one can further estimate the variance-covariance matrix of the dual ellipse parameters which is particularly meaningful. The 2x2 submatrix including  $D^*$ ,  $E^*$  and their covariance term, directly provides the uncertainty of the center coordinates. The development of the covariance expression is detailed in [15].

### 3.4 Algebraic error in the dual space

Dual conic and point conic share a strong relationship in the representation of the algebraic error. The relationship comes from the equivalence of the error expressions under a conic matrix inversion. In the dual space, the error is proportional to the distance between a tangent  $l_i$  and its pole  $x_i = \mathbf{C}^* l_i$  whereas, in the normal space, the error is proportional to the distance between a point  $x_i$  and its polar  $l_i = \mathbf{C} x_i$ . The dual conic error is represented as  $\varepsilon_i$  in Fig.3(a). Also, for both the conic and dual conic, the algebraic error evolves differently as the Euclidean distance increases along the ellipse contour. This can be observed from the spacing between isocontours in Fig.3(b) and Fig.3(c), which is different for regions of low and high curvature. In the figure, the



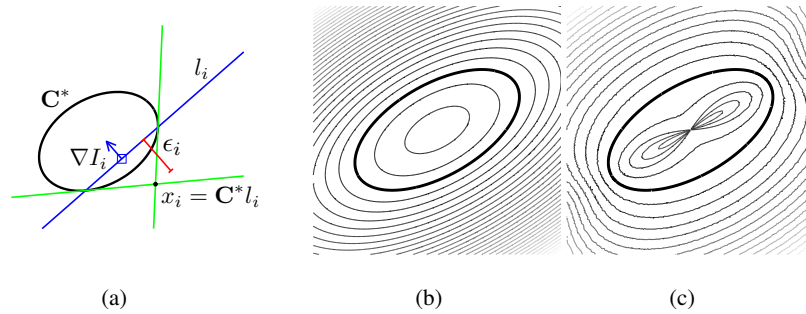


**Fig. 3** Algebraic error. (a) In the dual space, the algebraic error is proportional to the distance  $\epsilon$ . (b) Isocontours of the point conic error. (c) Isocontours of the dual conic error.

bold line marks the ellipse position. To produce the plot in Fig.3(c), the algebraic error is computed at each point using the tangent sampled from a set of concentric ellipses.

For point conics, the spacing between isocontours is larger, both at the extremities and inside the ellipse. This results in overestimating the ellipse size and eccentricity [16]. In Fig.3(c), the opposite phenomenon can be observed for the dual ellipse. In this case, the ellipse size and eccentricity are underestimated. While the bias is not significant when dealing with full ellipses, estimation from partial contours magnifies the bias. The dual ellipse operator will generally be more affected than a point based operator. Actually, the operator includes data overlapping the complete transition region of the ellipse edge which can extend over several pixels, depending on the size of the gradient operator. These pixels largely contribute to bias the solution, even in absence of noise. This will be demonstrated in the experiments section. Nevertheless, the bias can be reduced given a renormalization method [12] to correctly reweigh the observations.

## 4 Experiments

Three experiments were carried out to compare the new dual ellipse operator to other approaches. First the accuracy of the operator is assessed and compared in simulation on complete ellipses. In this part, the ground truth enables any bias of the operator to be uncovered. Then, the repeatability in presence of noise is analyzed along with the sensitivity to varying lighting conditions by processing images of a calibration target. Next, we assess the operator on partial contours and images taken from real world scenarios where occlusion and overlapping ellipses are present. In the first two experiments, the proposed operator is compared to the original Forstner operator for circular features (FCO), to the gray-scale centroid and to an efficient point ellipse fitting

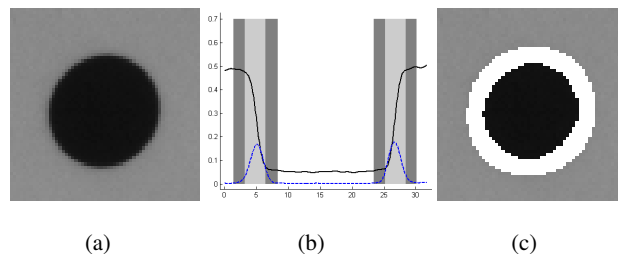








**Fig. 4** Region identification procedure of the operators for target images ((a)). In (b), a threshold is applied on the magnitude of the gradient. The solid lines represent the intensity value of the image and the dashed lines depict the gradient magnitude. The selected region, displayed in light gray, is then doubled by dilation to encompass the complete edge transition. The resulting region is shown superimposed on the image in (c).

method [10]. In this last method, the edge points of the feature are detected and their positions are refined to subpixel precision [9]. An ellipse is then estimated from the points with a direct least square fitting procedure that imposes an ellipse constraint [3]. To show the importance of subpixel correction, the results for ellipse estimation from the uncorrected local-maxima points are also included. It is important to note that the FCO and centroid methods only extract the feature center. The experiments focus on the center estimation but the dual ellipse method also extracts the complete set of parameters. When it is required for a given approach, the image gradient is calculated using a 5x5 Gaussian derivative filter.

In the experiments, the detection is decoupled from the localization. The dual ellipse and FCO operators could process all pixels in a region enclosing the ellipse, e.g. a bounding box. However, this remains valid as long as the ellipse is the only structure within the region. In the case of precise measurement applications such as camera calibration, all images contain contrasting features thus producing a high signal to noise ratio. This creates a clear bimodal distribution of the gradient magnitude. Therefore, setting an automatic threshold on the gradient magnitude [14] results in a coarse identification of the ellipse boundary. The complete procedure for the identification of ellipses is illustrated in Fig. 4. For the accuracy, repeatability and robustness experiments, the contributing regions were identified following this procedure. For instance, point ellipses were estimated from edges belonging to these regions. In the case of the centroid, the complete ellipse surface should contribute to the estimation hence the central area of the region was added.

**Table 1** Error on the center estimation (in pixels) for five methods applied at six noise levels.

						
Noise level	0%	2%	4%	6%	8%	10%
	<i>Mean (Max)</i>	<i>Mean (Max)</i>	<i>Mean (Max)</i>	<i>Mean (Max)</i>	<i>Mean (Max)</i>	<i>Mean (Max)</i>
<i>DualEllipse</i>	0.002 (0.005)	0.009 (0.023)	0.019 (0.047)	0.027 (0.077)	0.038 (0.109)	0.052 (0.125)
<i>PointEllipse</i>	0.007 (0.015)	0.011 (0.027)	0.020 (0.055)	0.029 (0.078)	0.042 (0.123)	0.061 (0.149)
<i>PointEllipse</i> <sup>1</sup>	0.167 (0.310)	0.165 (0.309)	0.165 (0.300)	0.166 (0.289)	0.171 (0.294)	0.166 (0.343)
<i>Centroid</i>	0.011 (0.027)	0.018 (0.053)	0.031 (0.099)	0.045 (0.134)	0.056 (0.130)	0.066 (0.178)
<i>FCO</i>	0.073 (0.180)	0.121 (0.402)	0.237 (0.789)	0.305 (0.673)	0.411 (1.256)	0.495 (1.529)

<sup>1</sup> Without subpixel correction

#### 4.1 Accuracy

In simulation, synthetic gray-scale images of ellipses are created with their actual positions precisely known. The pixel intensities of the synthetic images are set inversely proportional to their areas inside the actual ellipse before smoothing using a Gaussian filter of  $\sigma = 0.5$ . Next, the images are contaminated with additive Gaussian noise with standard deviation increasing from 0 to 10 percent of the image range. For each noise level, the mean and max error of the ellipse position are evaluated on 150 different images. Actually, besides adding noise, a different ellipse is generated in each image. The ellipse center coordinates, axes and angle are generated randomly. While the ellipse center coordinates are restricted to lie within a 5.0 pixel radius of the image center, the axes and angle of the ellipse vary randomly within the range  $[5.0, 15.0]$  pixels and  $[-\pi/2, \pi/2]$  radian respectively. The positioning errors are compiled in Table 1. The top row includes sample images to give a qualitative appreciation of the noise.

The simulation results indicate that FCO is the most sensitive to noise. In fact, although it exploits the set of local edges, it does not impose the more global constraint of an ellipse geometric model. Furthermore, noise is amplified due to the distance between the estimated ellipse center and the edges. Although the results are not included here, the experiment was in fact repeated with circular features where the ellipse axes were set equal. As expected, the FCO error was reduced by an average of 15% but it is still far from the precision

of the best methods. Since the gray-scale centroid method averages over all pixels of the feature, it shows high immunity to noise, but it preserves a higher error. The dual ellipse operator is the most accurate in all conditions. However, as noise increases, the estimation of the gradient orientation becomes less precise and the dual ellipse and subpixel point ellipse methods present similar accuracy with a small, but systematic advantage for the dual ellipse method. The high error obtained from ellipse fitting on raw points is due to a random leap of position of the local maxima caused by image noise. This confirms the importance of an accurate subpixel correction step before an ellipse can be estimated. Finally, the distribution of the error vectors confirmed the absence of bias for all of the operators.

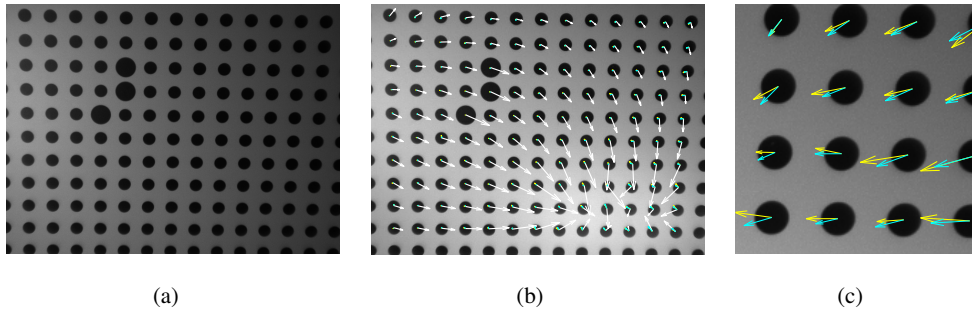
#### 4.2 Repeatability and robustness to non-uniform illumination

The second part of the experiments aims to assess the repeatability of the operator and its robustness to lighting variations in real conditions. In this experiment, the positions of the ellipses are unknown so we can only compare the variation of position of the detected centers when varying illumination. For that purpose, two sequences of 150 images of a planar calibration target comprising a set of circles are acquired (see Fig. 5). The camera and calibration target are set fixed to an optical table mounted on pneumatic vibration isolators so both are perfectly still. The images were captured with a firewire camera at a resolution of 640x480 pixels. Each image contains 130 low eccentricity ellipses with mean diameter of approximately 30 pixels. In order to measure repeatability, we computed the mean and maximum ellipse displacements in the first sequence. Both are listed in the first row of Table 2.

The second image sequence is acquired under different lighting conditions. To accomplish this, a new light source is added to the scene before capturing the sequence. The addition of a new light creates a visible change of illumination and prevents any setup manipulation between the two acquisitions. The effect of the added light source can be observed in Fig. 5(b). Special care was taken to use high frequency fluorescent lamps (300hz) having the same color spectrum to avoid any feature displacement due to chromatic aberration or flickering. The displacement is taken as the distance between the mean center of a given ellipse in the first sequence to its mean center in the second sequence. The mean and maximum displacements of the ellipses between the two sequences are listed in the bottom row of Table 2.

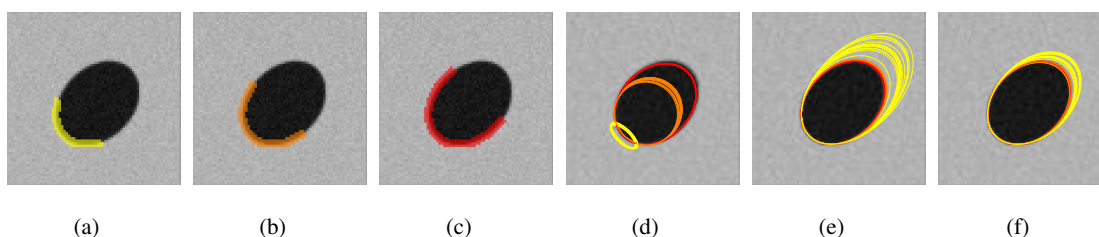
**Table 2** Ellipse center variations under noise (top) and shift under lighting variation (bottom) in real imaging conditions.

	<i>DualEllipse</i>	<i>PointEllipse</i>	<i>PointEllipse</i> <sup>1</sup>	<i>Centroid</i>	<i>FCO</i>
	<i>Mean (Max)</i>	<i>Mean (Max)</i>	<i>Mean (Max)</i>	<i>Mean (Max)</i>	<i>Mean (Max)</i>
Ellipse center variation (pixels)	0.009 (0.015)	0.008 ( 0.014 )	0.020 ( 0.045 )	0.010 ( 0.017 )	0.057 ( 0.081 )
Displacement magnitude (pixels)	0.009 (0.025)	0.008 ( 0.027 )	0.010 ( 0.033 )	0.069 ( 0.145 )	0.229 ( 0.493 )

<sup>1</sup> Without subpixel correction

**Fig. 5** Displacement due to lighting variation. (a) The calibration target under initial lighting conditions. (b) A sample image under new lighting conditions with superimposed arrows showing the direction and magnitude of the ellipse displacement amplified 400x for centroid (white), dual conic (yellow) and point conic with subpixel correction (cyan). The results of FCO were the most affected and were omitted for clarity. (c) Close-up of a region showing only the dual conic and point conic errors, amplified 2500x.

From the first sequence, the experimental results are consistent with those obtained in simulation. Indeed, in the presence of noise, the centroid, dual ellipse and point ellipse with subpixel correction methods show a higher precision than the FCO and point ellipse methods. In the second sequence, the addition of a new light source changes the intensity profile of the ellipses. An operator which integrates on a large surface area is more likely to be affected by this phenomenon. A direct consequence of this is the strong displacement observed for the centroid approach. The displacement is systematic toward the new brighter image region as depicted in Fig. 5(b). This confirms that the centroid is not a reliable localization approach unless conditions are well controlled. Still, the change of intensity will also affect the gradient magnitude along the ellipse contour. Thus, we might expect different results between the point ellipse and dual ellipse methods as only the latter weighs each observation with the gradient magnitude. Interestingly, the orientation of the displacement vectors in



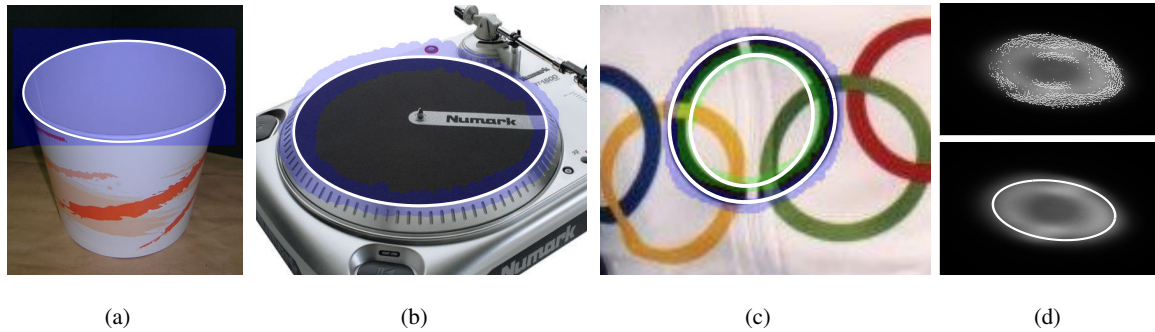
**Fig. 6** Analysis of ellipse estimation from partial contours. Ellipses are estimated from data included in regions covering three percentages of the contour, (a) 25%, (b) 50% and (c) 75%. The estimation is performed 15 times for each coverage percentage on images contaminated with Gaussian noise having  $\sigma = 2\%$  of the image range. The results are given for (d) dual ellipse operator, (e) dual ellipse operator with renormalization and (f) point conic with renormalization. In these images, the ellipse colors correspond to the region colors in (a), (b) or (c).

Fig. 5(c) and their magnitudes in Table 2 are very similar. The gradient magnitude variations do not penalize the dual ellipse operator which behaves as well as the best point conic method in these conditions.

#### 4.3 Application to partial ellipses and natural images

Although the dual ellipse operator was developed for the estimation of complete ellipses from calibration targets, it is interesting to study its behavior on partial ellipses and appreciate its stability. To accomplish this, a simulation is performed where ellipses are estimated from contiguous partial contours. Ellipses are estimated from regions covering three different percentages of the contour, as illustrated in Fig.6 (a) to (c). To simulate real conditions, the images are contaminated with Gaussian noise having  $\sigma = 2\%$  of the image range. The experiment is repeated 15 times for each coverage percentage using three estimation methods, namely, (d) dual ellipse, (e) dual ellipse with renormalization and (f) point conic with renormalization.

The dual ellipse fitting is affected when the coverage is below 50%; Fig.6(d) confirms the presence of the low eccentricity bias. Still, the slow and constant progression toward a small ellipse suggests that the operator degrades gracefully as coverage is reduced. Interestingly, the estimation can be easily improved by applying a renormalization step based on the idea exposed in [12]. The ellipses obtained after renormalization are displayed in Fig. 6(e). The bias was greatly reduced, particularly when more than 50% of the ellipse contour was covered. However, given smaller coverage, noise becomes prevalent in the estimation which results in less reliable results. The experiment was also performed with the subpixel point conic method with renormalization. The resulting ellipses, displayed in Fig. 6(f), are closer to the original contour, even when



**Fig. 7** Examples of estimation from natural images. (a) Coffee cup. (b) Turn table. (c) Olympic rings. (d) Spotlight superimposed with the gradient local maxima (top) and the dual ellipse (bottom). In (a) to (c), the ellipses are estimated from the colored regions segmented manually whereas in (d), the ellipse is estimated from the entire image.

the coverage is small. Estimation from points appears to be more reliable when the coverage is very limited, given that the extracted points closely follow the original ellipse contour.

To further appreciate the stability of the operator, estimations are performed from natural images. In these images, the operator encounters overlapping ellipses, outliers and incomplete contours. Since the purpose of the operator is to estimate ellipses and not to detect them, regions where the operator is applied are roughly segmented by hand. By proceeding this way, we ensure that a region mostly overlaps a single ellipse. The selected regions are displayed as colored shades in Fig.7.

Weighting each observation with the squared gradient magnitude improves the stability of the operator. This is particularly apparent in Fig.7(a), where the ellipse was estimated from a large bounding box area. Although the estimation is not formally robust, the method is still applicable in the presence of outliers. For example, the ellipse estimated from the turn table in Fig.7(b) properly follows the selected contour with strong contrast but also with perpendicular marks nearby the contour. However, in difficult cases where outliers have equally strong gradients, the estimation may be affected. This is shown in Fig.7(c), where the overlapping rings were deliberately selected to be part of the estimation regions. In addition to the presence of outliers, the ellipse contours in Fig.7(c) are also incomplete. In this particular case, the observations are distributed all along the ellipse contour with some missing data or outliers. This is a different type of partial contour compared with Fig.6.

In the previous examples, the ellipse contours are sharp and well defined. However, in images having a low contrast or bad focus, meaningful edge points can hardly be extracted. In such a situation, point conic methods are not applicable. An example is given in Fig.7(d). The image was obtained by aiming a desktop spotlight to

a planar surface which created a blurry and non-uniform image. The local maxima of the gradient, obtained after applying a threshold, are scattered on the entire ellipse surface and do not belong to a well defined contour. This can be observed on the top image of the figure. Still, the global structure of an ellipse is present. Since the operator exploits the active zone of the gradient, the region of application does not need to be well defined. In this case, the operator processed the entire image and was able to identify the elliptic spotlight, as shown on the bottom image of the figure.

## 5 Conclusion

The new linear operator combines the advantages of the most precise ellipse fitting methods with the simplicity of the Forstner operator as well as its capability to work on the raw image gradient. The operator presents low sensitivity to noise as well as to non uniform illumination. While the latter advantage stems from exploiting the gradient information, its immunity to noise arises from averaging over pixels in the neighborhood of the ellipse's edges while weighing with the squared gradient magnitude. The absence of precise contour point extraction makes it faster and simpler than point conic methods and allows the uncertainty of the parameters to be evaluated directly from the raw gradient image. This is particularly useful for camera calibration. Furthermore, the operator efficiently constrains the dual conic to a dual ellipse when minimizing the algebraic error.

More robust estimation techniques can also be easily applied in replacement of the least-squares if that were necessary for a given application. For example, the dual ellipse operator benefits from the renormalization procedure in the presence of partial contours, a procedure initially developed for point conic estimation. Since the operator can estimate an ellipse from entire image regions, an interesting research avenue would consist in investigating this kind of more direct method for detection as well.

## References

1. Bookstein, F.L.: Fitting conic sections to scattered data. *Computer Graphics and Image Processing* **9**(1), 56–71 (1979)
2. Cabrera, J., Meer, P.: Unbiased estimation of ellipses by bootstrapping. *IEEE Trans. on Pattern Analysis and Machine Intelligence* **18**(7), 752–756 (1996)
3. Fitzgibbon, A., Pilu, M., Fisher, R.B.: Direct least square fitting of ellipses. *IEEE Trans. on Pattern Analysis and Machine Intelligence* **21**(5), 476–480 (1999)



4. Fitzgibbon, A.W., Fisher, R.B.: A buyer's guide to conic fitting. In: Proceedings of the 6th British conference on Machine vision, vol. 2, pp. 513–522. BMVA Press (1995)
5. Forstner, W., Gulch, E.: A fast operator for detection and precise location of distinct points, corners and centres of circular features. In: Proc. Intercommission Conf. on Fast Processing of Photogrammetric Data, pp. 281–305 (1987)
6. Gander, W., Golub, G.H., Strebler, R.: Fitting of circles and ellipses, least square solution. Tech. Rep. 1994TR-217, ETH Zurich, Institute of Scientific Computing (1994)
7. Hartley, R.I.: In defense of the eight-point algorithm. *IEEE Trans. on Pattern Analysis and Machine Intelligence* **19**(6), 580–593 (1997)
8. Hartley, R.I., Zisserman, A.: *Multiple View Geometry in Computer Vision*, second edn. Cambridge University Press, ISBN: 0521540518 (2004)
9. Heikkila, J.: Moment and curvature preserving technique for accurate ellipse boundary detection. In: Proceedings of the 14th International Conference on Pattern Recognition, vol. 1, p. 734. IEEE Computer Society, Washington, DC, USA (1998)
10. Heikkila, J.: Geometric camera calibration using circular control points. *IEEE Trans. on Pattern Analysis and Machine Intelligence* **22**(10), 1066–1077 (2000)
11. Kanatani, K.: *Geometric computation for machine vision*. Oxford University Press, Inc., New York, NY, USA (1993)
12. Kanatani, K.: Statistical bias of conic fitting and renormalization. *IEEE Trans. on Pattern Analysis and Machine Intelligence* **16**(3), 320–326 (1994)
13. Kanatani, K.: Ellipse fitting with hyperaccuracy. *IEICE - Trans. Inf. Syst.* **E89-D**(10), 2653–2660 (2006). DOI <http://dx.doi.org/10.1093/ietisy/e89-d.10.2653>
14. Otsu, N.: A threshold selection method from gray-level histograms. *IEEE Trans. on Systems, Man, and Cybernetics* **9**(1), 62–66 (1979)
15. Ouellet, J.N., Hebert, P.: A simple operator for very precise estimation of ellipses. In: CRV '07: Proceedings of the Fourth Canadian Conference on Computer and Robot Vision, pp. 21–28. IEEE Computer Society, Washington, DC, USA (2007)
16. Rosin, P.L.: Assessing error of fit functions for ellipses. *Graphical models and image processing: GMIP* **58**(5), 494–502 (1996)
17. Safaee-Rad, R., Tchoukanov, I., Benhabib, B., Smith, K.C.: Accurate parameter estimation of quadratic curves from grey-level images. *CVGIP Image Understanding* **54**(2), 259–274 (1991)
18. Szeliski, R., Kang, S.B.: Direct method for visual scene reconstruction. In: Proceedings of the IEEE Workshop on Representation of Visual Scenes, pp. 26–33. IEEE Computer Society, Washington, DC, USA (1995)
19. Tabatabai, A., Mitchell, O.: Edge location to subpixel values in digital imagery. *IEEE Trans. on Pattern Analysis and Machine Intelligence* **6**(2), 188–200 (1984)
20. Trucco, E., Verri, A.: *Introductory Techniques for 3-D Computer Vision*. Prentice Hall PTR, Upper Saddle River, NJ, USA (1998)